Meat Science 86 (2010) 780–793

Contents lists available at ScienceDirect

Meat Science

journal homepage: www.elsevier.com/locate/meatsci

Theoretical analysis on pulsed microwave heating of pork meat supported on ceramic plate

Tanmay Basak *, Badri S. Rao

Department of Chemical Engineering, Indian Institute of Technology Madras, Chennai 600036, India

ARTICLE INFO

Article history:
Received 24 July 2009
Received in revised form 2 June 2010
Accepted 22 June 2010

Keywords:
Microwave heating
Pulsing
Pork meat
White Pudding
Pork Luncheon Roll

ABSTRACT

Theoretical analysis has been carried out to study the role of ceramic plates (alumina and SiC) and pulsed microwave heating of pork meat (Pork Luncheon Roll (PLR) and White Pudding (WP)) samples. Spatial hot spots occur either at the center of the sample or at the outer face or at the face attached with alumina plate and application of pulsing minimizes formation of hot spots within meat samples. Pulsing of microwave is characterized by set point for temperature difference (ΔT_S) and on–off constraints for temperature (T'). It is found that alumina plate with higher ΔT_S and lower T' may be recommended for thick meat samples (both WP and PLR) whereas for thin meat samples, lower ΔT_S with alumina plate/without plate may be preferred. It is also observed that SiC plate may be selectively used with $\Delta T_S = 20$ K for both the pork meats. The distributed microwave incidence is found to be effective due to lesser degree of thermal runaway in absence of pulsing for both meat samples.

1. Introduction

Microwaves are electromagnetic waves in the frequency range of 300 MHz to 300 GHz. During microwave propagation, electromagnetic waves pass through the material. The accompanying transport process based on interaction between microwaves and material particles result in dissipation of electric energy into heat throughout the entire material volume. Based on volumetric heating effects, microwave heating has several advantages such as brief startup, internal heating, high efficiency and rapid processing over conventional heating (Ayappa, Davis, Crapiste, Davis, & Gordon, 1991; Chatterjee, Basak, & Ayappa, 1998; Gunasekaran & Yang, 2007a; Kwon, Belanger, Pare, & Yaylayan, 2003; McMinn, Khraisheh, & Magee, 2003; McMinn, 2004; Wang et al., 2006). Because of industrial demand, microwave are useful for cooking, heating, drying, pasteurizing, sintering and food processing (Alajaji & El-Adawy, 2006; Ayappa, Davis, Crapiste, et al., 1991; Bonafonte, Iglesias, & Bueno, 2007; Garg & Mendiratta, 2006; Gunasekaran & Yang, 2007a; Jeong et al., 2007; Lyng, Cronin, Brunton, Li, & Gu, 2007; McMinn et al., 2003; McMinn, 2004; Rodriguez, Penazzi, Caboni, Bertscco, & Lercker, 1997; Serrano, Librelotto, Cofrades, Sanchez-Muniz, & Jimenez-Colmenero, 2007). It may be important to note that microwave assisted cooked food is as nutritious as food cooked by other means and research suggests that microwave cooking retains more vitamins, minerals and nutrients compared to conventional heating (Alajaji & El-Adawy, 2006).

A number of earlier works are based on experimental and theoretical investigations on microwave heating of food substances (Ayappa, Davis, Crapiste, et al., 1991; Ayappa, Davis, Davis, & Gordon, 1991, 1992; Barringer, Davis, Gordon, & Ayappa, 1995; Basak & Kumaran, 2005; Campanone & Zaritzky, 2005; Chen, 1998; Damez & Clerjon, 2008; Jeong et al., 2007; Lin, Anantheswaran, & Puri, 1995; McKenna, Lyng, Brunton, & Shirsat, 2006; McMinn, 2004; McMinn et al., 2003; McMinn, 2006; Oliveira & Franca, 2002; Zhang, Lyng, Brunton, Morgan, & McKenna, 2004). The microwave heating of food substances is fundamentally based on sample dimensions, multilayered slab processing, multiphase heating and material dielectric properties (Ayappa, Davis, Crapiste, et al., 1991; Ayappa, Davis, Davis, et al., 1991; Ayappa et al., 1992; Basak & Priya, 2005; Basak & Meenakshi, 2006a,b; Bhattacharya & Basak, 2006; Brunton, Lyng, Zhang, & Jacquier, 2006; Farag, Lyng, Morgan, & Cronin, 2008; Lyng, Zhang, & Brunton, 2005; Vasanthi, Venkataramanujam, & Dushyanthan, 2007; Zhang et al., 2004). Zhang et al. (2004) found that the dielectric and thermophysical properties of pork meat (White Pudding, WP and Pork Luncheon Roll, PLR) are temperature dependent and they measured the properties in the temperature range of 5–85 °C.

Modeling on microwave processing for food materials has been developed by earlier researchers (Ayappa, Davis, Crapiste, et al., 1991; Ayappa, Davis, Davis, et al., 1991; Ayappa et al., 1992; Barringer et al., 1995; Basak & Priya, 2005; Basak & Meenakshi, 2006a; Bhattacharya & Basak, 2006; Campanone & Zaritzky, 2005; Curet, Rouaud, & Boillereaux, 2008; Hill & Marchant, 1996; Khraisheh, Cooper, &

* Corresponding author. Tel.: +91 44 2257 4173; fax: +91 44 2257 0509.
E-mail address: tanmay@iitm.ac.in (T. Basak).

0309-1740/$ – see front matter © 2010 The American Meat Science Association. Published by Elsevier Ltd. All rights reserved.
doi:10.1016/j.meatsci.2010.06.021

Magee, 1995; Liu, Wang, & Sakai, 2005; Ng et al., 2008; Ohlsson & Bengtsson, 1971; Oliveira & Franca, 2002; Regier, Housova, & Hoke, 2001; Wang & Sun, 2003; Yang & Gunasekaran, 2004). Maxwell's Equation or Lambert's exponential law for microwave propagation and energy balance with a volumetric source term due to propagation of microwaves form the basis of the theoretical models on microwave assisted transport processes.

Oliveira and Franca (2002) compared temperature distribution in food samples based on Maxwell's Equations and Lambert's Law and found that the sample size within the Lambert's Law limit is higher for cylinders as compared to slabs. According to Lambert's Law, microwave power decays exponentially as a function of distance of penetration into the sample (Ohlsson & Bengtsson, 1971) but this law is theoretically less applicable for simulating the microwave power (Liu et al., 2005) whereas Maxwell's Equation is based on space and time dependence and that characterizes the exact behavior of microwave propagation (Ayappa, Davis, Crapiste, et al., 1991; Ayappa, Davis, Davis, et al., 1991; Ayappa et al., 1992; Barringer et al., 1995; Bhattacharya & Basak, 2006; Curet et al., 2008). Note that, internal standing waves based on Maxwell's Equations depict the exact variation in temperature distribution even for small sample variation (Barringer et al., 1995). Bhattacharya and Basak (2006) have studied comprehensively on microwave power absorption and associated heating characteristics for various food materials. They have established a closed form solution for prediction of resonating sample lengths based on distributed microwave incidence for optimal heating strategy. Curet et al. (2008) reported that resonance phenomena are observed experimentally in the frozen product and this can only be predicted using Maxwell's Equations, not by Lambert's Law.

The temperature distribution during microwave heating has earlier been studied for variety of food products by several researchers (Gunasekaran & Yang, 2007b; Oliveira & Franca, 2002; Ramaswamy & Pilletwill, 1992; Taher & Farid, 2001; Yang & Gunasekaran, 2001, 2004; Yarmand & Homayouni, 2009). Ramaswamy and Pilletwill (1992) reported that microwave heating causes uneven temperature distribution or surface over heating within food sample. The major drawback associated with microwave heating is the non-uniform temperature distribution within the sample, resulting in hot spots, cold spots and edge or surface overheating. Yang and Gunasekaran (2001, 2004) reported that the non-uniform temperature distribution during continuous microwave heating may be reduced when pulsed microwave heating was used. However, pulsed microwave heating increases the processing time but the power absorption into the samples are same for continuous and pulsed microwave incidence. To increase the processing rate and simultaneously to reduce the thermal runaway, optimized pulse microwave may be used. Gunasekaran and Yang (2007b) reported that, the constraint (ΔT_{on}) is very critical for optimum heating and they concluded that $\Delta T_{on}=20$ °C may be a better choice than $\Delta T_{on}=15$ °C for mashed potatoes. However, thermal runaway depends on dielectric and thermal properties of the material and sample dimension. Minimization of thermal runaway based on temperature distribution and power absorption within the sample is a critical issue.

Current work is an attempt to analyze microwave heating dynamics of two meat batters such as White Pudding (WP) and Pork Luncheon Roll (PLR). Motivation of this work is based on earlier studies as reported by Zhang et al. (2004) and that study reported complete characterization on thermal and dielectric properties of WP and PLR. Till date, a detailed theoretical investigation on microwave heating of meat batters based on the realistic or experimental data on thermal and dielectric properties is yet to appear in the literature. Current work proposes microwave heating of meat slabs with or without supporting ceramic plates and the theoretical predictions may provide guideline for optimal heating of meat samples in presence of uniform plane wave. Zhang et al. (2004) demonstrated that dielectric properties are functions of temperature. Further, McKenna et al. (2006) reported that dielectric constant and dielectric loss for WP show maxima at 45 °C whereas dielectric constant and dielectric loss for PLR exhibit maxima at 65 °C. These data further imply that dielectric losses attain maxima at specific temperatures and a larger value of dielectric loss also corresponds to larger power absorption. Large heat generation within meat samples at specific locations may lead to hot spot which further deteriorate the quality of food. Therefore, simulation studies have also been carried out to investigate heating dynamics with minimization of thermal runaway using on–off control or pulsed microwave incidence within meat samples.

Current simulations are aimed to demonstrate the heating strategy of meat samples (WP and PLR) attached with ceramic support or plate via continuous as well as pulsed microwave incidences. The ceramic plates (Alumina or SiC) have been used as alumina is transparent to microwave and SiC absorbs microwave significantly. Hence, the choice of these two ceramic layers may give exact guideline for the effect of support on microwave processing of food samples. The optimal thermal runaway is an important issue for meat processing and the distribution of microwave incidences at both sides with pulsing may play critical role for efficient meat processing. Various sample thicknesses have been identified based on processing time (t_p) vs. sample thickness (L_s) and thermal runaway (ΔT_p) vs. sample thickness (L_s) for continuous and pulsed microwave incidences. The thermal characteristics and heating rates are obtained via energy balance equation with volumetric source term due to microwaves. We have analyzed the influence of ceramic plates and pulsed microwave incident intensities in presence of various distributions of microwave incidence for efficient processing of meat samples. The effect of optimized pulsing on various case studies of microwave heating of meat samples has also been studied in detail.

2. Modeling and simulation

2.1. Electric field in a composite slab

Microwaves are assumed to be uniform plane electromagnetic waves. Electric and magnetic fields lie in x–y plane and vary in the direction of propagation (z-axis) as shown in Fig. 1a–b. Current study involves sample with/without supporting plate. Lateral dimensions (along x and y axes) are assumed to be very large compared to the total thickness of sample (along z-axis including ceramic layer) and similar modeling assumptions are also found in earlier literatures (Ayappa, Davis, Crapiste, et al., 1991; Ayappa et al., 1992; Basak & Priya, 2005; Basak & Meenakshi, 2006a,b). Based on the assumptions, one dimensional slab has been considered. The wave propagation due to uniform electric field (E_x), given by Maxwell's Equation is

$$\frac{d^2E_x}{dz^2} + \kappa^2(T)E_x = 0, \tag{1}$$

where E_x lies in x–y plane. In Eq. (1), $\kappa(T) = \frac{\omega}{c}\sqrt{\kappa'(T) + i\kappa''(T)}$ is the propagation constant which depends on dielectric constant, $\kappa'(T)$ and dielectric loss, $\kappa''(T)$. Note that, $\omega = 2\pi f$ where f is the frequency of the electromagnetic wave and c is the velocity of light.

The dielectric properties ($\kappa'(T)$ and $\kappa''(T)$) of both WP and PLR correspond to the frequency of 2.45 GHz. Zhang et al. (2004) reported the experimental data on dielectric properties of meat and based on the data, the polynomial fittings of dielectric properties for WP and PLR have been obtained in this work. Fig. 2a and b illustrate comparison of dielectric data of WP and PLR (Zhang et al., 2004) and a fourth order polynomial fit based on current work agrees well with experimental predictions (Zhang et al., 2004). The coefficients in polynomial fittings of dielectric properties for WP and PLR are given in

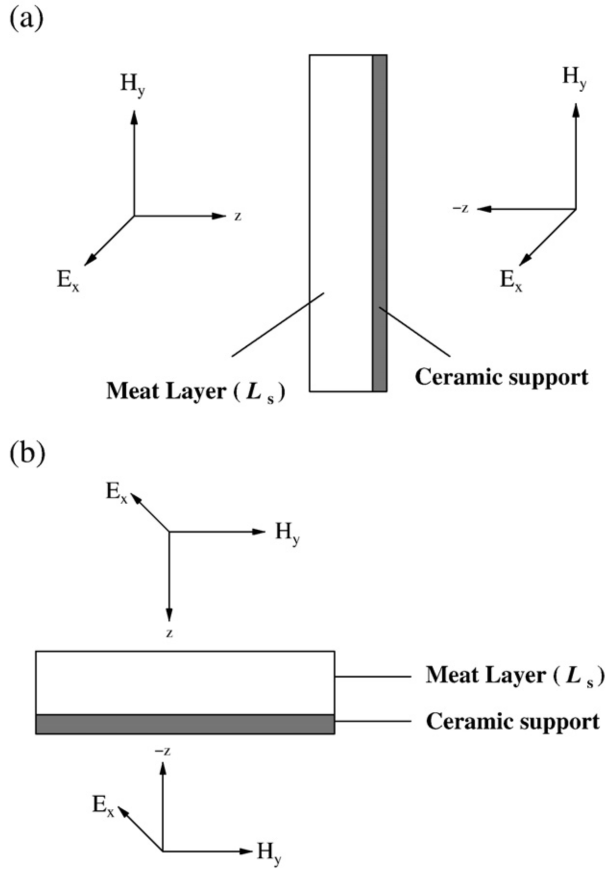

(c)

Case 1	**Continuous microwave incidence**
Case 2	**ΔT_s = 10 K**
Case 3	**ΔT_s = 20 K**

Fig. 1. Schematic illustration of sample exposed to plane electromagnetic wave: (a) schematic for model system (b) schematic for a practical application where sample is kept with a ceramic support exposed to uniform plane waves incident either from top or from top as well as bottom and (c) the chart for setpoint of temperature difference (ΔT_S) corresponding to cases 1–3.

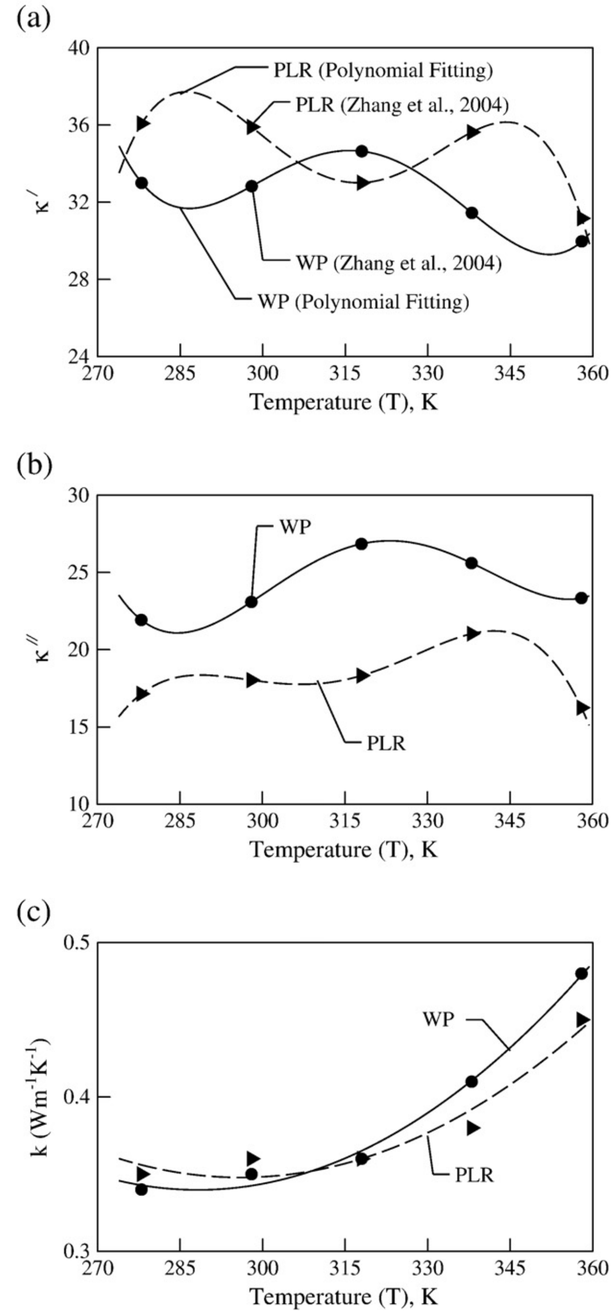

Fig. 2. (a) Dielectric constant (κ'), (b) dielectric loss (κ'') and (c) thermal conductivity (k, W m$^{-1}K^{-1}$) vs. temperature (T, K) for White Pudding (WP) and Pork Luncheon Roll (PLR). Note that the symbols (WP, •; PLR, ►) denote experimental data (Zhang et al., 2004) and polynomial fitting is represented by continuous curves (WP, —; PLR, ———).

Table 1. It may be noted that dielectric properties are assumed to be constant for $T \geq 358$ K based on trend in the experimental data. The dielectric properties for ceramic materials (alumina and SiC) are also reported in Table 1.

The meat sample, ceramic support and or layer constitute a multilayer slab which is subjected to microwave as seen in Fig. 1a, b. In an n multilayered sample, the electric field for l^{th} layer obtained from Eq. (1) is

$$\frac{d^2E_{x,l}}{dz^2} + \kappa_l^2(T)E_{x,l} = 0, \tag{2}$$

where $z_{l-1} \leq z \leq z_l$ and $l = 1 \ldots n$. The boundary conditions at the interface are,

$$\left.\begin{aligned} E_{x,l} &= E_{x,l+1} \\ \frac{dE_{x,l}}{dz} &= \frac{dE_{x,l+1}}{dz} \end{aligned}\right\} \quad \begin{aligned} l &= 1 \ldots n-1 \\ z &= z_1 \ldots z_{n-1}, \end{aligned} \tag{3}$$

Here $z_1, z_2 \ldots z_{n-1}$ denote the interface positions. The boundary conditions at the outer face of the composite slab are (Ayappa, Davis, Crapiste, et al., 1991; Ayappa et al., 1992; Basak & Priya, 2005; Basak & Meenakshi, 2006a,b),

$$\frac{dE_x}{dz} + ik(T)E_x = 2ik(T)E_L e^{-ik(T)L}, \quad z = z_1 = -L \tag{4}$$

and

$$\frac{dE_x}{dz} - ik(T)E_x = -2ik(T)E_R e^{-ik(T)L}, \quad z = z_n = L \tag{5}$$

Table 1
Dielectric and thermophysical properties (Ayappa et al., 1992; Chatterjee et al., 1998; Zhang et al., 2004).

$P = a_0 + a_1T + a_2T^2 + a_3T^3 + a_4T^4$, ($T$ in Kelvin).					
Property	Variables	WP ($T \le 358$ K)	PLR ($T \le 358$ K)	Alumina	SiC
Dielectric constant $P = \kappa'$	a_0	35792.261	−53,038.269	10.8	26.66
	a_1	−454.2723467	677.9089		
	a_2	2.1566221	−3.2375398		
	a_3	−4.53446E-3	6.851985E-3		
	a_4	3.5625926E-06	−5.422716E-6		
Dielectric loss $P = \kappa''$	a_0	31,213.077	−31,740.064	0.1566	27.99
	a_1	−393.43678	409.22056		
	a_2	1.853108	−1.972854		
	a_3	−3.862822E-3	4.21706E-3		
	a_4	3.00716E-6	−3.371852E-06		
Specific heat, $P = C_p$ (J Kg^{-1} K^{-1})	a_0	3033.6	3474.8	1046	3300
Thermal conductivity, $P = k$ (W m^{-1} K^{-1})	a_0	2.716	2.5399		
	a_1	−0.01648533	−0.01481033	26	40
	a_2	2.85933E-05	2.501667E-05		
Density, ρ (Kg m^{-3})	a_0	931.88	800.95	3750	3100

Pulsing of microwave heating is carried out via estimating temperature difference within samples (ΔT_p), which is defined as

$$\Delta T_p = T_{max} - T_{min} \tag{6}$$

where T_{max} and T_{min} are maximum and minimum temperature of meat sample, respectively. The pulsing is done in the following manner. Microwave source is switched on if

$$\Delta T_p \le \Delta T_S - T', \tag{7}$$

and the source is switched off if

$$\Delta T_p \ge \Delta T_S + T'. \tag{8}$$

Hence, the power absorption in l^{th} layer (either meat sample or ceramic),

$$q_l(z,T) = \frac{1}{2}\omega\varepsilon_0\kappa_l(T)E_{x,l}(z)E^*_{x,l}(z), \Delta T_p \le \Delta T_S - T', \forall l. \tag{9}$$

$$= 0, \quad \Delta T_p \ge \Delta T_S + T', \forall l. \tag{10}$$

where * denotes the complex conjugate, ΔT_S and T' are the setpoint for temperature difference and on–off constraint respectively. Note that, setpoint (ΔT_s) is the desired value of ΔT_p which has to be maintained and on–off constraint (T') controls the duration of power cycle. Note that, T' is the variable which decides the upper and lower bounds of the setpoint. Efficiency of pulsing is quantified by Pulsing ratio (PR) which is defined as

$$PR = \frac{t_{off}}{t_p} \tag{11}$$

where t_{off} and $t_p = t_{on} + t_{off}$ are overall power off time and total processing time, respectively.

2.2. Modeling microwave heating

Heat transport in a dielectric material during microwave radiation is due to a combined effect of volumetric heat generation and conduction. The unsteady state one dimensional energy balance equation for microwave heating is

$$\frac{\partial H}{\partial t} = \frac{\partial}{\partial z}\left[k(T)\frac{\partial T}{\partial z}\right] + q(z,T), \tag{12}$$

where

$$H = \rho C_p(T)(T - T_0). \tag{13}$$

Note that, ρ, $C_p(T)$, T_0, $k(T)$ and $q(z,T)$ are the density, specific heat, initial temperature, thermal conductivity and volumetric heat generation, respectively. The thermal properties for WP and PLR are taken from the experimental results of Zhang et al. (2004). The temperature dependent properties are obtained from polynomial fittings, and coefficients of polynomial functions are given in Table 1. Fig. 2c illustrates that polynomial fitting of thermal conductivity of WP and PLR agree well with experimental data (Zhang et al., 2004). The values of specific heat for WP and PLR are taken as the average of experimental data of Zhang et al. (2004) whereas density for WP and PLR are calculated based on the ratio of thermal conductivity to the product of thermal diffusivity and specific heat data of earlier work (Zhang et al., 2004). Rahman (1995) reported that specific heat of fresh pork meat is in the range of 3054–3431 kJ/kg C whereas the values used for WP and PLR are 3033.6 and 3474.8, respectively. The estimated density values for WP and PLR are 931.88 and 800.95 Kg m^{-3} respectively, being very similar to those reported by Sanz, Alonso, and Mascheroni (1987). The thermal properties of ceramics layers (Al_2O_3 and SiC) are assumed to be constant within the temperature range considered in simulation based on earlier work (see Table 1; Chatterjee et al., 1998).

The energy balance equation for l^{th} layer in n multilayered sample consisting of pork meat samples and ceramics is represented as

$$\frac{\partial H_l}{\partial t} = \frac{\partial}{\partial z}\left[k_l(T)\frac{\partial T_l}{\partial z}\right] + q_l(z,T), \quad l = 1 \ldots n \tag{14}$$

The initial condition is

$$T_l = T_0, \quad l = 1 \ldots n \tag{15}$$

and the boundary conditions are

$$k_1(T)\frac{\partial T_1}{\partial z} = h(T_1 - T_\infty), \quad z = z_1 \tag{16}$$

and

$$-k_{n-1}(T)\frac{\partial T_{n-1}}{\partial z} = h(T_{n-1} - T_\infty), \quad z = z_{n-1} \tag{17}$$

The interface conditions between various layers are

$$\left.\begin{aligned} T_l &= T_{l+1} \\ k_l(T)\frac{\partial T_l}{\partial z} &= k_{l+1}(T)\frac{\partial T_{l+1}}{\partial z} \end{aligned}\right\} \begin{aligned} &l = 2 \ldots n-2 \\ &z = z_2 \ldots z_{n-2} \end{aligned} \tag{18}$$

Microwave power, $q_l(z,T)$ is a function of electric field and temperature as given in Eq. (9). The nonlinear coupled wave propagation and energy balance equation (Eqs. (2) and (14)) with appropriate boundary and interface conditions (Eqs. (3)–(5) and (16)–(18)) are solved simultaneously using similar procedure as discussed by earlier works (Ayappa, Davis, Davis, et al., 1991; Basak & Priya, 2005; Basak & Meenakshi, 2006a,b).

2.3. Materials, methods and numerical parameters

The microwave heating in multilayered slabs with temperature dependent dielectric and thermal properties is modeled with coupled Maxwell Equation (Eq. (2)) and energy balance equation (Eq. (14)). The coupled equations with appropriate boundary conditions are simultaneously solved with Galerkin finite element method. Crank–Nicholson method is used to discretize the time domain, and the non linear residual equations are solved using Newton Raphson Method. Due to the lack of a good initial guess to begin the Newton scheme, a small time step $\Delta t = 1 \times 10^{-4}$ s was used at the first time step. Unless specified otherwise $\Delta t = 0.5$ s was used for subsequent steps. Typically, 25–50 quadratic elements (15–35 elements for meat sample and 10–15 elements for ceramic layer) were used for entire slab. It was found that the maximum difference for the values of the unknowns at the nodes was less than 1% when the values were compared for 25 and 50 elements. For constant dielectric properties, analytical solution of Eq. (2) is available (see Basak & Priya, 2005) and the power distribution can be obtained without solving the energy balance equation (Basak & Priya, 2005). The validation of current simulation strategy is done by comparing the power distribution with the available analytical/numerical solution for materials with constant and temperature dependent dielectric properties (Ayappa, Davis, Crapiste, et al., 1991; Ayappa, Davis, Davis, et al., 1991).

The assembly consists of pork meat (WP and PLR) sample layer with ceramic plate (Al_2O_3 or SiC) as supports on one side and the thickness of the ceramic layer is considered as 0.2 cm. The support is placed in the right face of the meat sample as seen in Fig. 1a, b. The analysis is carried out for one side as well as both sides microwave incidence as seen in Fig. 1a and b. The intensities of radiation from left and right sides are 3 W cm^{-2} and 0 W cm^{-2} for one side incidence, respectively whereas they are 1.5 W cm^{-2} and 1.5 W cm^{-2} for both sides incidence. The detailed analysis is carried out based on continuous and pulsed microwave incidences with parameters enlisted in Fig. 1c. The heat transfer coefficient at the outer faces is assumed to be 2 W m^{-2} K^{-1} for all computations. The initial temperature of the samples (including ceramic layer) is 300 K. In this study, the setpoint for temperature difference (ΔT_S) is considered as 10 and 20 K. The on–off constraint (T') is considered to be 1, 2 and 5 K and these values are representative cases for switching on–off during microwave pulsing. The simulation results are shown up to the time at which average temperature reaches 350 K for pork meat samples (WP and PLR).

3. Results and discussion

3.1. Processing characteristics for White Pudding (WP)

A preliminary study has been carried out to illustrate the distributions of processing time (t_p) and thermal runaway (ΔT_p) characteristics vs. sample thickness (L_s) for one side and both sides microwave incidence in presence of various ceramic supports as shown in Fig. 3a–f. The time to reach average temperature being 350 K within the sample may be defined as processing time (t_p) and the temperature difference (T_{max}–T_{min}) within the sample is a measure of thermal runaway (ΔT_p). The processing time (t_p) and thermal runaway (ΔT_p) vs. sample thickness (L_s) diagrams are important to further analyze efficient meat processing at greater heating rates with uniform temperature distribution within the sample. The prime objective of these diagrams (Fig. 3a–f) is to identify specific sample thicknesses for optimal processing conditions based on t_p and ΔT_p values.

Fig. 3a and b illustrate the variations for t_p and ΔT_p vs. sample thickness (L_s) in absence of any support due to one side and both sides incidence, respectively. It may be noted that, processing without pulsing corresponds to case 1 and pulsing corresponds to cases 2 and 3. It may also be noted that cases 1–3 are outlined in Fig. 1c and T' is considered as 2 K for this study. It is observed from Fig. 3a that t_p is an increasing function till $L_s = 0.7$ cm and thereafter local minima occurs and further, t_p is found to be an increasing function with L_s. An increasing trend of t_p vs. L_s is also observed for $L_s \geq 1$ cm with cases 2 and 3 for no supports (Fig. 3a, b). Note that, t_p for one side incidence is larger than that for both sides incidence with cases 2 and 3. It is also interesting to observe that ΔT_p for case 3 is larger than that for case 2, but t_p for case 3 is smaller than for case 2 in all situations. Common to all these cases, it is observed that ΔT_p is a sharp increasing function of L_s especially for $L_s \geq 0.5$ cm with one side incidence and for $L_s \geq 1.5$ cm with both sides incidence involving case 1 (no pulsing) only. Application of pulsing drastically reduces ΔT_p for cases 2 and 3. However, ΔT_p is found to have smaller magnitudes for $L_s \leq 1$ cm. Qualitatively similar distributions for t_p and ΔT_p are observed for alumina and SiC supports for one side and both sides microwave incidences (Fig. 3c–f). Therefore it is worthwhile to investigate further in detail spatial heating and pulsing characteristics for representative sample thicknesses. The test cases are shown for $L_s \leq 1.5$ cm based on less t_p and ΔT_p.

Fig. 4a–c illustrate the spatial distributions of power and temperature for WP sample corresponding to $L_s = 1.5$ cm due to one side microwave incidence. Note that, the analysis is carried out with $T' = 2$ K for cases 2 and 3. It is observed that maxima in microwave power occurs near the exposed face and minima occurs near the unexposed face with/without pulsing cases and similar qualitative trend in power absorption occurs for with/without supporting plates. Note that, the maximum in microwave power occurs due to constructive interference whereas the minimum is due to destructive interference of traveling waves. It is important to note that, dielectric properties are assumed to be constant for $T \geq 358$ K based on dielectric data as reported by Zhang et al. (2004) and therefore, microwave power distribution is invariant with/without pulsing for supports/without supports cases at t_p corresponding to $T = 350$ K.

Common to all situations with/without supporting plates, temperature has a maxima near the exposed face and the minima occur at the unexposed face attached with ceramic support. It is interesting to observe that the temperature near the exposed face varies around 385–388 K and that near the unexposed face varies around 308–320 K without pulsing (case 1) with/without supporting plates. In contrast, the temperature of meat sample varies within 343–356 K for case 2 with/without support whereas the range is 338–360 K for case 3 with/without support. It is interesting to note that, pulsing minimizes the thermal runaway (see third column of Fig. 4a–c) and the processing

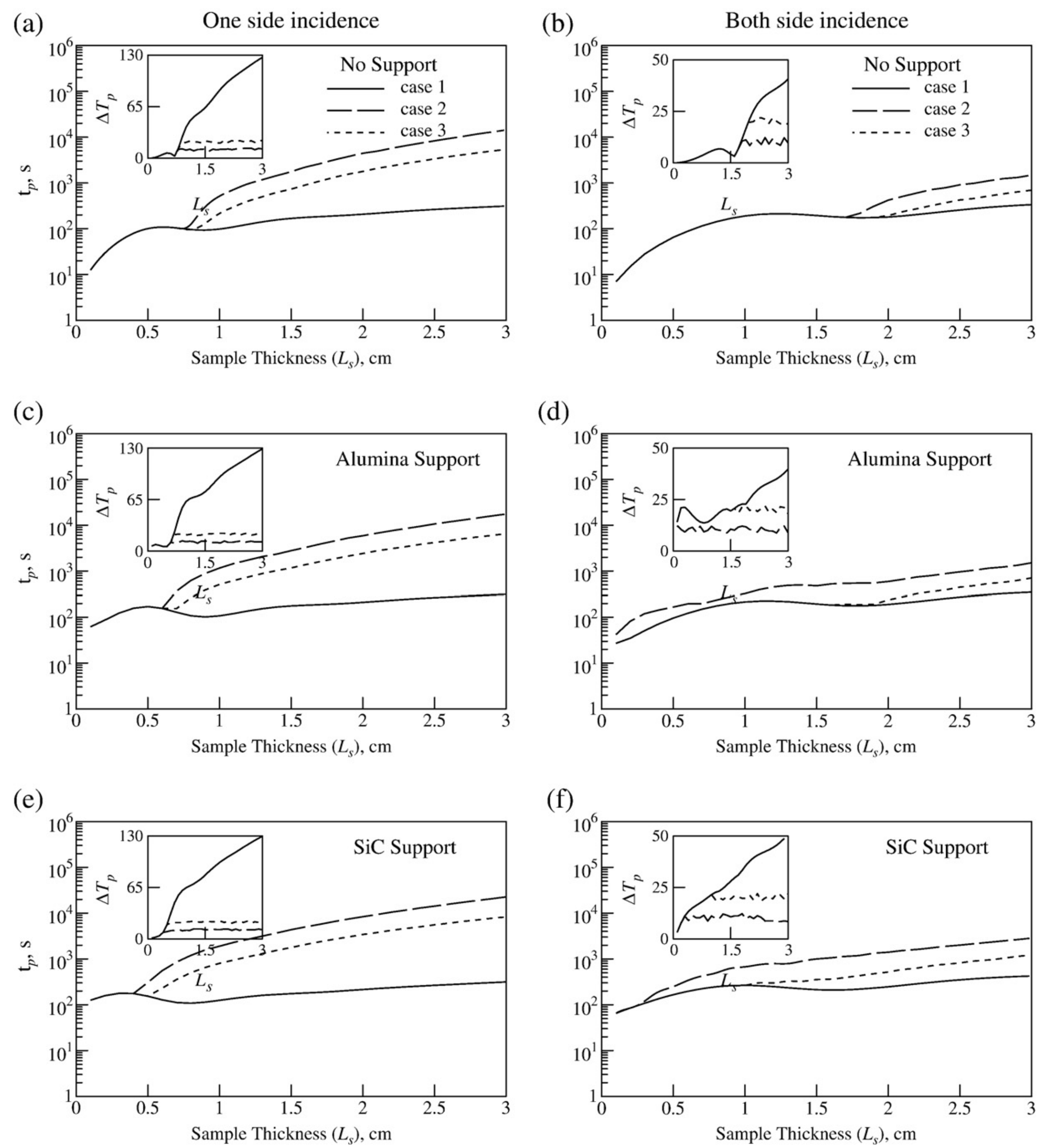

Fig. 3. Processing time (t_p) and temperature difference (ΔT_p) vs. sample thickness (L_s) diagrams for cases 1–3, corresponding to without plate, alumina and SiC plates for White Pudding (WP) due to one side (a, b and c) and both sides (d, e and f) incidence. $I_L = 3$ W cm^{-2}, $I_R = 0$ (for one side incidence), $I_L = 1.5$ W cm^{-2}, $I_R = 1.5$ W cm^{-2} (for both sides incidence), $f = 2450$ MHz, $T' = 2$ K.

time (t_p) is found to be smallest without any support. On the other hand, t_p is largest with SiC plate especially with cases 2 and 3. Thermal runaway is in general less for cases 2 and 3, but that sharply increase with time for case 1. This clearly indicates that pulsing is important to achieve uniform heating within WP sample and one may operate either with case 2 or case 3 based on optimal thermal runaway situations.

Fig. 5a–c illustrate the spatial distributions of power and temperature for WP sample corresponding to $L_s = 1.5$ cm due to both sides incidence and the analysis is carried out with $T' = 2$ K for cases 2 and 3. It is observed that maxima in microwave power occurs at both the faces as well as at the center whereas minima occurs near the one-fourth of distance from both faces with/without pulsing cases and similar qualitative trend in power absorption occurs with/without supporting plates. In contrast to one side incidence, processing time (t_p) is drastically reduced for both sides incidence with cases 2 and 3.

Common to all situations with/without supporting plates, temperature has a maxima near the exposed face as well as at the center whereas minima occurs near one forth distance from the faces of the meat samples. It is interesting to observe that the temperature near left face is around 353–361 K and that near the ceramic plate is around 334–344 K with supporting plates (Fig. 5b, c). On the other hand, the temperature was found to vary within 348–352 K throughout the sample for cases 1–3 without support (Fig. 5a). Although pulsing minimizes the thermal runaway (see third column of Fig. 5b and c), but the processing time (t_p) is found to be smallest without any support and t_p is largest for SiC plate. In contrast, t_p for cases 1–3

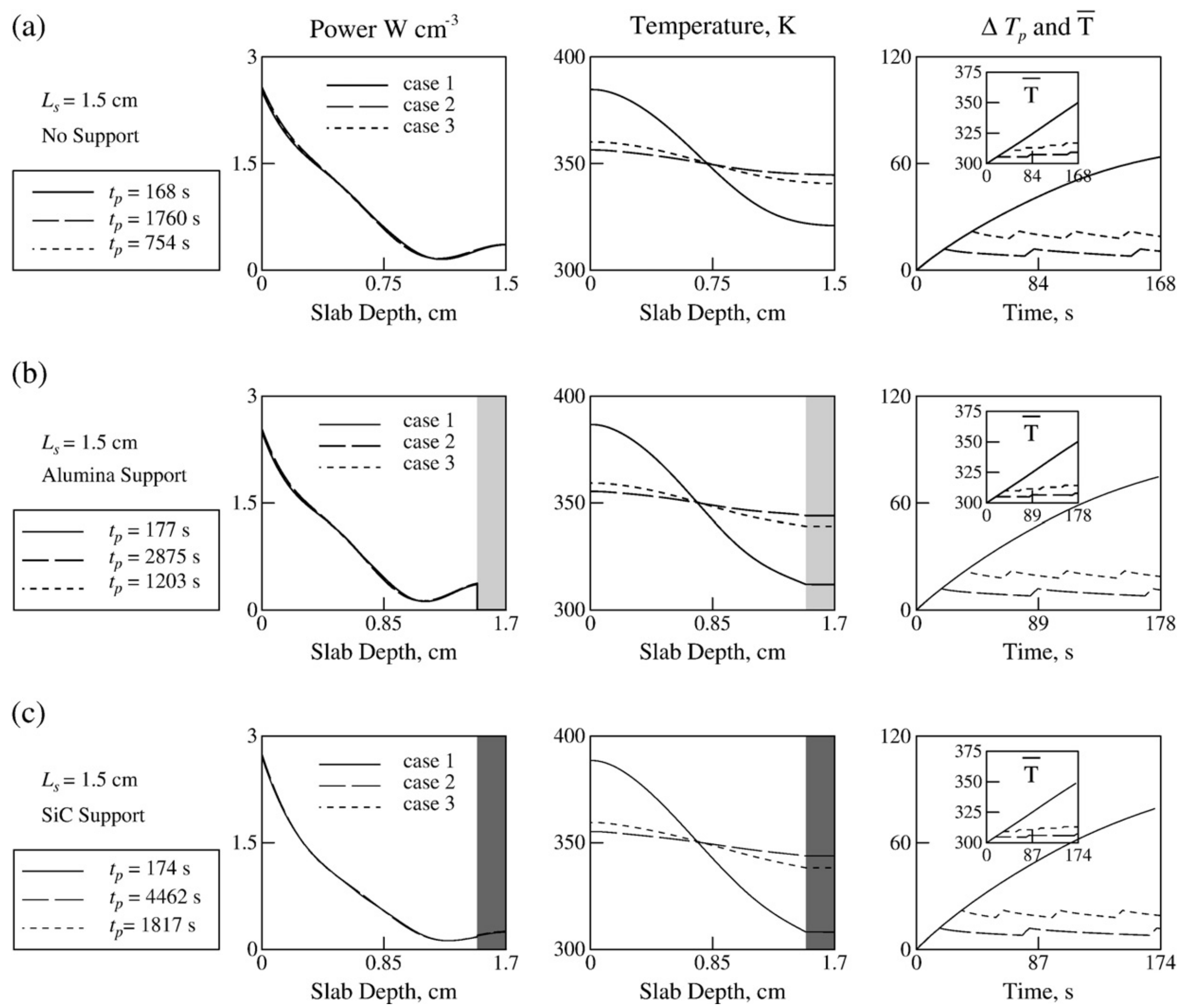

Fig. 4. Spatial power distributions (first column), temperature profiles (second column), temperature difference (ΔT_p) vs. time (t) (third column) and average temperature ($\overline{T}$) vs. time (t) (inset plots in third column) for cases 1–3, corresponding to $L_s = 1.5$ cm due to one side incidence for White Pudding (WP) samples; (a) without plate, (b) alumina plate and (c) SiC plate. $f = 2450$ MHz, $I_L = 3$ W cm^{-2}, $I_R = 0$, $T' = 2$ K.

without any support are identical (see Fig. 5a). It is interesting to note that the uniform temperature distribution is observed within the sample without any supporting plate. The uniform temperature distribution is also attributed with lowest degree of thermal runaway. Due to uniform temperature distribution, t_p with cases 1–3 are identical as seen in Fig. 5a. Overall, alumina plate may be a preferred as supporting plate based on optimal value of t_p and degree of thermal runaway for one/both side incidence case.

3.2. Characteristics of pulse cycle for WP

The effects of on–off constraint (T'), setpoint (ΔT_s) and sample thickness (L_s) on power cycle are discussed in this section. Fig. 6a–c illustrate microwave pulse cycles for various thicknesses ($L_s = 0.5$, 1 and 1.5 cm) with three different sets of T' (1, 2 and 5 K) for $\Delta T_s = 10$ K corresponding to one side incidence. Note that, this study is carried out for samples without any ceramic support and the effect of T' on sample with support may be discussed in a similar manner. It is interesting to observe that the average temperature of WP sample reaches 350 K for $L_s = 0.5$ cm before the pulsing starts for all values of T' (Fig. 6a).

Fig. 6b illustrates pulse cycle for $L_s = 1$ cm. It may be noted that the processing time for $T' = 1$ K, $T' = 2$ K and $T' = 5$ K are 503 s, 514 s and 544 s respectively. At $T' = 1$ K, it is observed that the total power on time (t_{on}) is 102 s and power off time (t_{off}) is 401 s whereas for $T' = 2$ and 5 K, t_{on} are 103 s (identical for $T' = 2$ and 5 K) and t_{off} are 411 s and 441 s, respectively. It is also interesting to note that, as T' increases, frequency of pulsing decreases. It may be important to note that, power on time (t_{on}) is almost invariant with constraint (T') whereas power off time (t_{off}) increases with T'.

The power cycles for $L_s = 1.5$ cm (see Fig. 6c) are qualitatively similar to that of $L_s = 1$ cm, as seen in Fig. 6b. It may be noted that the processing time for $T' = 1$ K, $T' = 2$ K and $T' = 5$ K are 1764 s, 1760 s and 1916 s, respectively. At $T' = 1$ K, it is observed that the total power on time (t_{on}) is 184 s and power off time (t_{off}) is 1580 s whereas for $T' = 2$ and 5 K, t_{on} are 184 s and 185 s and t_{off} are 1576 s and 1731 s, respectively. As mentioned for $L_s = 1$ cm case, the frequency of pulsing decreases with T'. It may be important to note that, power on time (t_{on}) is also invariant with constraint (T') whereas power off time (t_{off}) increases significantly with T'. Similar analysis has also been carried out for $\Delta T_S = 20$ K (figures not shown). The pulse cycle with larger values of ΔT_S is found to be qualitatively similar to that of Fig. 6a–c and the total power on time is invariant with setpoint and the total power off time decreases as the setpoint increases. Consequently, as the setpoint increases, the processing time reduces, which is a direct consequence of increase in initial power on duration.

Fig. 7a and b illustrate overall pulse ratio (PR) for various sample thicknesses ($L_s = 0.5 - 1.5$ cm) without ceramic support corresponding to various ΔT_s and T' due to one side and both sides incidence, respectively. Note that, overall pulse ratio (PR) is defined as the ratio of

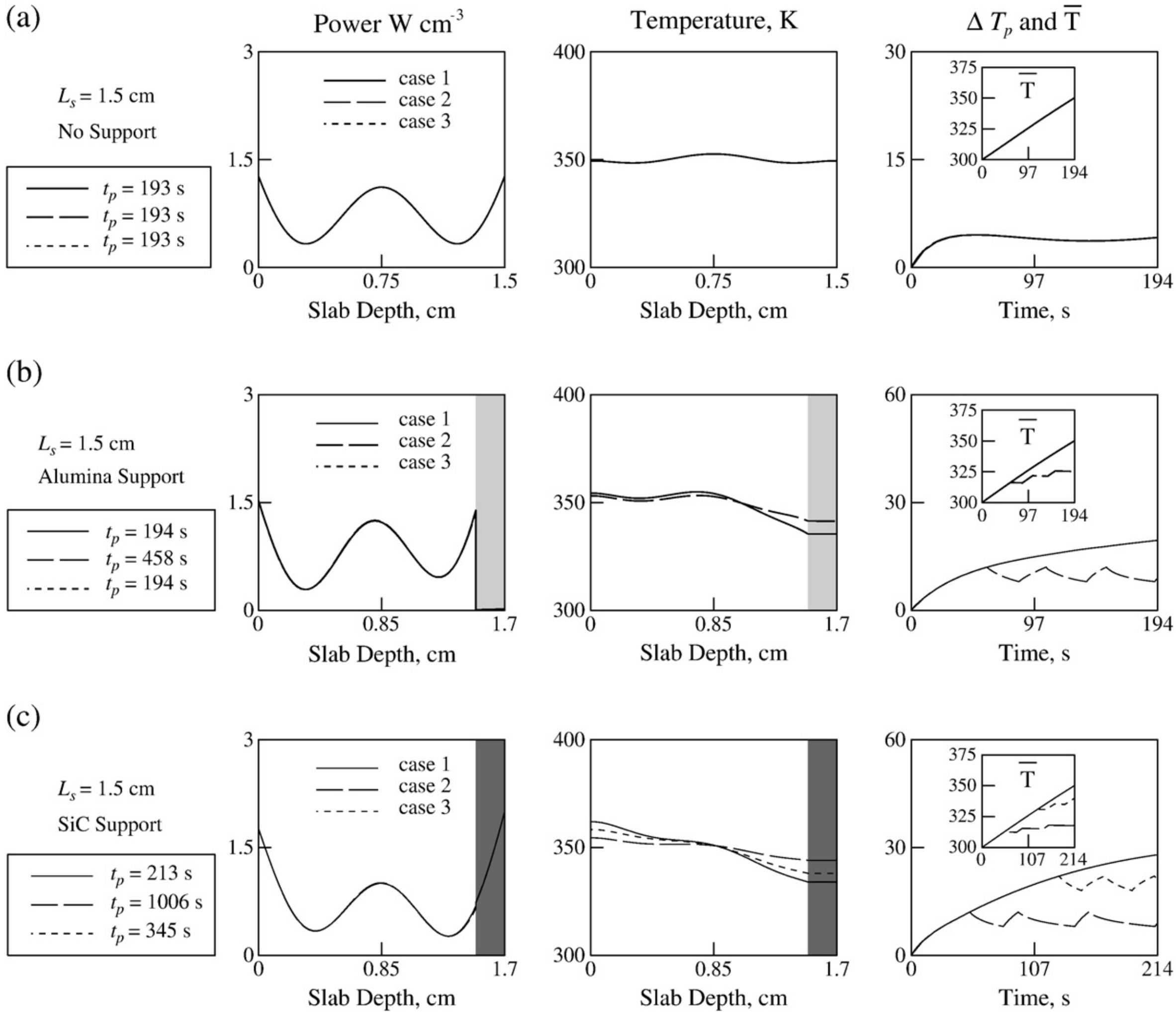

Fig. 5. Spatial power distributions (first column), temperature profiles (second column), temperature difference (ΔT_p) vs. time (t) (third column) and average temperature ($\overline{T}$) vs. time (t) (inset plots in third column) for cases 1–3, corresponding to $L_s = 1.5$ cm due to both sides incidence for White Pudding (WP) samples; (a) without plate, (b) with alumina plate and (c) SiC plate. $f = 2450$ MHz, $I_L = 1.5$ W cm^{-2}, $I_R = 1.5$ W cm^{-2}, $T' = 2$ K.

overall power off time (t_{off}) to processing time (t_p). Therefore, PR equals 0 if there is no pulsing and PR approaches to one if power is off for most of the time. Thus, PR around unity is not recommended due to high power off time leading to larger processing time. Fig. 7a demonstrates that PR for $L_s = 0.5$ cm is zero which signifies that no pulsing is required. In contrast, PR for $L_s = 1.5$ cm approaches to one and this may be due to high ΔT_p within the sample in absence of pulsing. Therefore, power is switched off most of the time as ΔT_p is much larger than 20 K (ΔT_S). It is observed that PR decreases with increase in setpoint (ΔT_S) for $L_s = 1 - 1.5$ cm. Fig. 7a shows that PR increases with increase in thickness of the sample during one side incidence whereas PR is found to be invariant (PR = 0) for all L_s during both sides incidence as seen in Fig. 7b. Overall, PR of any length scale corresponding to both sides incidence is less as compared to that of one side incidence. It may be important to note that PR being zero for both sides incidence is an indicative of less ΔT_p in absence of pulsing, and lesser ΔT_p with both sides incidence for smaller L_s ($L_s \leq 1.5$ cm) is also seen in Figs. 3b and 5.

Fig. 7c and d show variations of overall pulse ratio (PR) for samples attached with alumina support corresponding to various ΔT_s and T' due to one side and both sides microwave incidence, respectively. Fig. 7c shows that, PR for $L_s = 0.5$ cm is quite less which signifies pulsing is less significant. It is interesting to see that PR is almost invariant of ΔT_S and T' and this also denotes lower degree of thermal runaway for $L_s = 0.5$ cm. In contrast, PR is almost in unity for $L_s = 1$ and 1.5 cm. Fig. 7d displays PR for both sides incidence with alumina support. It is interesting to observe that, $L_s = 0.5 - 1.5$ cm correspond to lower PR, which is in contrast to one side incidence. On the other hand, PR of any length scale corresponding to both sides incidence with alumina support is larger than that of without support with both sides incidence as seen in Fig. 7b. Based on the analysis, it is interesting to note that sample without any support has lesser PR than that with alumina support during one side as well as both sides incidence for $L_s = 0.5 - 1.5$ cm for lower values of ΔT_S and this information is important to decide heating strategy.

Fig. 7e and f display variations of overall pulse ratio (PR) for samples attached with SiC support due to one side and both sides microwave incidences, respectively. Fig. 7e depicts that, PR for $L_s = 0.5$ cm has larger values than those in Fig. 7a and c whereas those of $L_s = 1 - 1.5$ cm are near to unity. Fig. 7f displays the distributions of PR for both sides incidence with SiC support. Similar to previous case studies, $L_s = 0.5 - 1.5$ cm has lesser PR values for both sides incidence than those for one side incidence. In general, PR for all lengths corresponding to one side or both sides incidence with SiC support is larger than PR for alumina or no support. Similar to previous cases (Fig. 7a–d), it is observed that $\Delta T_S = 20$ K also corresponds to lesser values of PR with one and both sides incidence. Thus samples attached with SiC plate may be optimally heated with both sides incidence corresponding to $\Delta T_S = 20$ K.

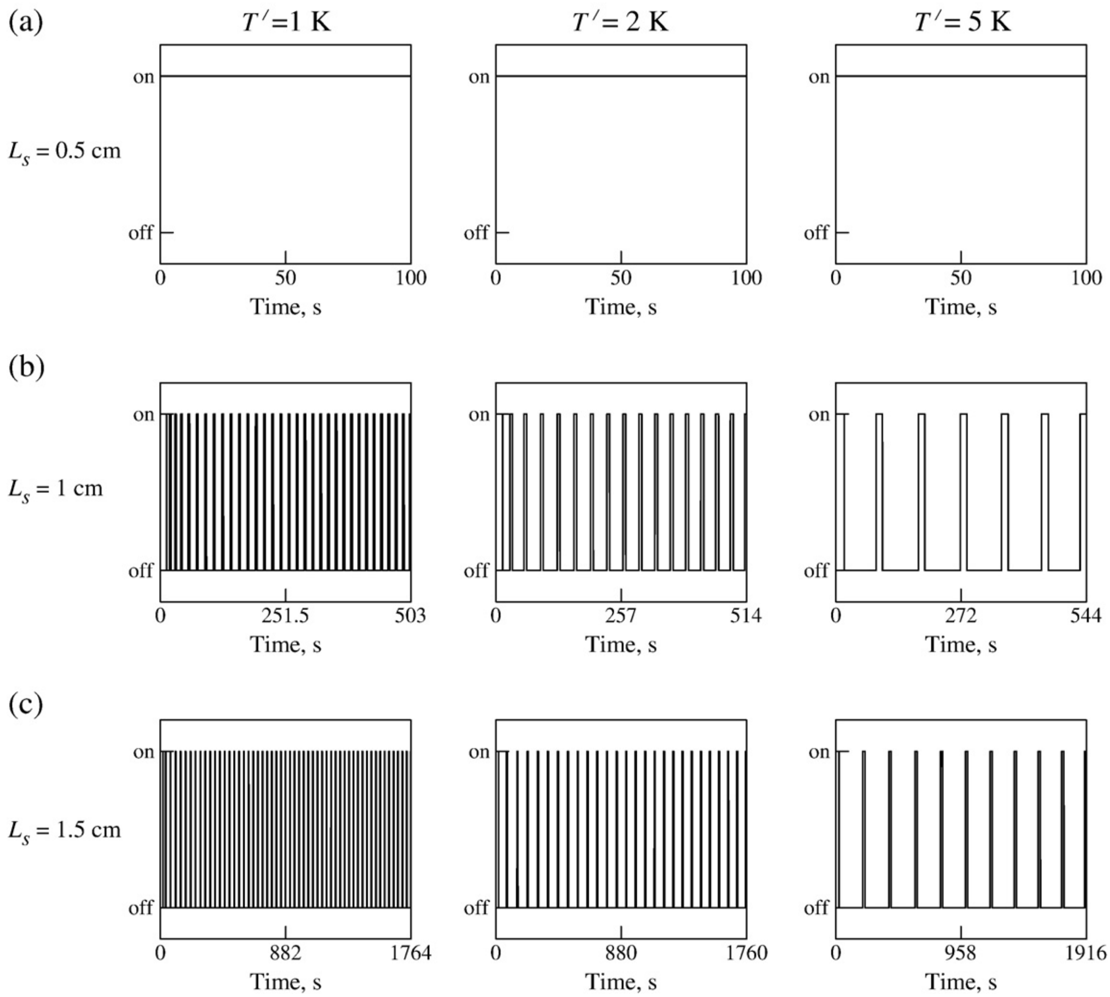

Fig. 6. Power cycle vs time (t) for White Pudding (WP) without any support due to one side incidence; (a) $L_s = 0.5$ cm, (b) $L_s = 1$ cm and (c) $L_s = 1.5$ cm. The three sets of on-off constraints: $T' = 1$ K (first column), $T' = 2$ K (second column) and $T' = 5$ K (third column). $f = 2450$ MHz, $I_L = 3$ W cm^{-2}, $I_R = 0$, $\Delta T_S = 10$ K.

3.3. Comprehensive remarks on efficient heating characteristics for WP

This section analyzes the role of optimized pulsing on efficient processing of WP sample with/without ceramic supports for three representative length scales. Note that, T' is considered as 2 K for this study. Fig. 8a–c illustrate the processing time (t_p), power on time (t_{on}) and temperature difference (ΔT_p) for all cases (cases 1–3) due to one side incidence. Fig. 8a shows that both processing time (t_p), power on time (t_{on}) are large for alumina support for $L_s = 0.5$ cm whereas smallest t_{on} is observed for samples without any support.

It is interesting to observe that t_{on} is almost identical with cases 1–3 for situations with no support or any support. Finally, it is observed that ΔT_p is minimum for alumina support irrespective of cases 1–3 and ΔT_p with no support has moderate values whereas ΔT_p is larger with SiC support. Therefore, either alumina support or no support with all cases (case 1–3) may be optimal choice for heating with support for $L_s = 0.5$ cm based on t_{on} and ΔT_p values.

Fig. 8b depicts that processing time (t_p), power on time (t_{on}) are largest for SiC support whereas samples without support correspond to smallest t_p and t_{on} for $L_s = 1$ cm. Although the processing time (t_p) varies considerably for all the cases with/without support, but the power on time (t_{on}) is almost invariant for all the cases with no support and alumina support, as seen in Fig. 8b. It is observed that, samples with alumina, SiC supports or without support with cases 2–3 have less thermal runaway as compared to case 1, but samples without supports with cases 2 and 3 have significantly less processing time as well as thermal runaway. It may be inferred that no support with case 2 or 3 may be suitable for $L_s = 1$ cm based on t_p, t_{on} and ΔT_p values.

Fig. 8c illustrates t_p, t_{on} and ΔT_p for $L_s = 1.5$ cm. Similar qualitative trend on t_p, t_{on} and ΔT_p for $L_s = 1.5$ cm and $L_s = 1$ cm corresponding to all cases with/without support have been observed (see Fig. 8b and c). Note that, processing time and power on time are largest for SiC support and smallest in absence of any support. It is interesting to observe that ΔT_p is significantly high with case 1 with/without support. It may also be noted that, processing time for $L_s = 1.5$ cm is in general larger than $L_s = 0.5$ and 1 cm with/without supports. It is also interesting to observe that ΔT_p has identical values for each of cases 2 and 3 with/without support. Overall, no support or alumina with case 3 may be the optimal choice for larger sample thicknesses based on smaller processing time (t_p) and ΔT_p.

3.4. Processing characteristics and efficient heating characteristics for Pork Luncheon Roll (PLR)

Processing time (t_p) and thermal runaway (ΔT_p) characteristics for one side and both sides microwave incidence have been analyzed as function of PLR sample thickness (L_s) in presence of various ceramic supports or no supports as shown in Fig. 9a–f. The prime objective of these diagrams (Fig. 9a–f) is to identify specific sample thicknesses for enhanced processing conditions based on t_p and ΔT_p values.

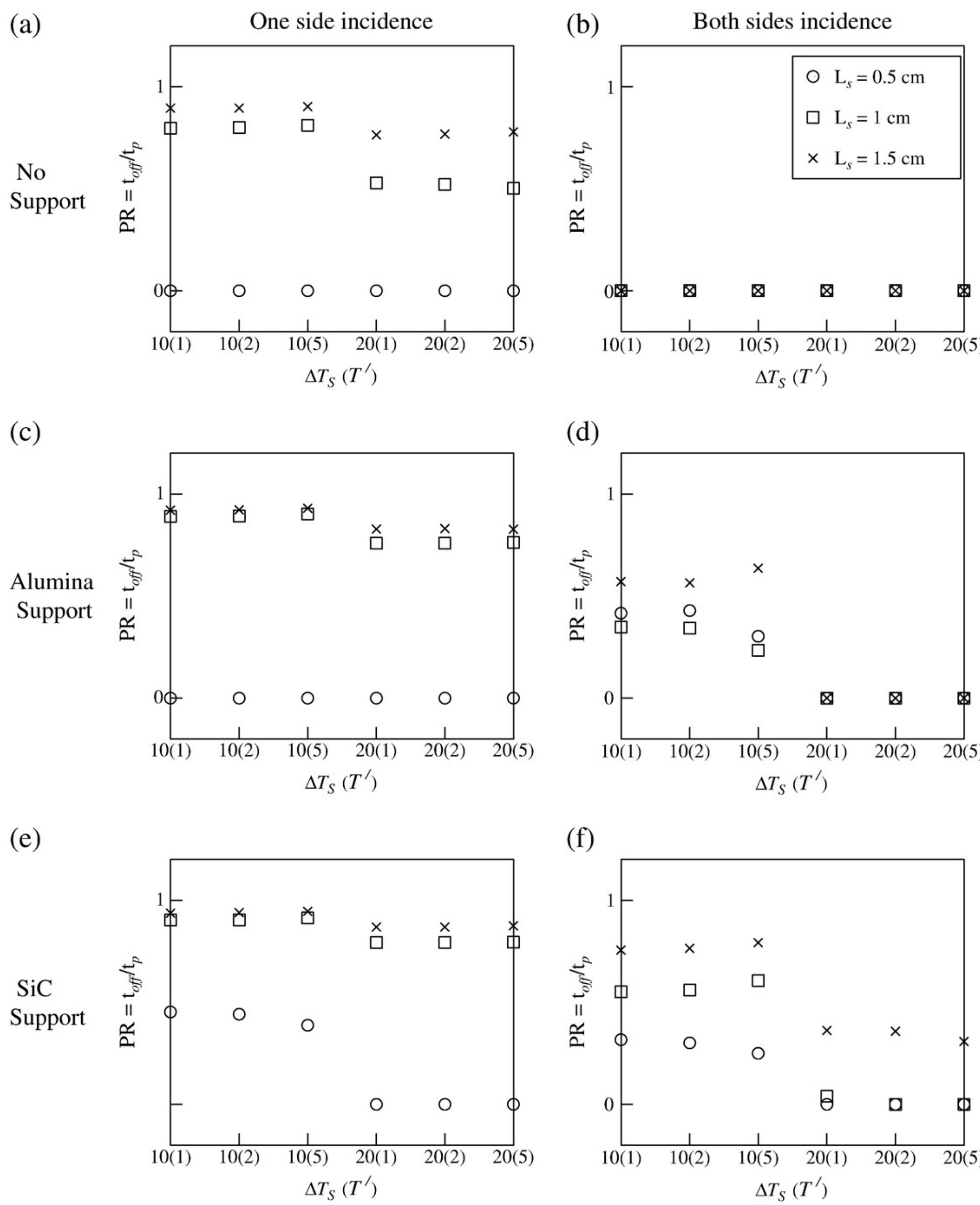

Fig. 7. Pulsing ratio (PR) vs setpoint (ΔT_S) and on–off constraint (T') for White Pudding (WP) samples corresponding to various length scales due to one side (a, c and e) and both sides (b, d and f) microwave incidence where (a) and (b) denote sample without plate; (c) and (d) denote sample attached with alumina plate; (e) and (f) denote sample attached with SiC plate. $I_L = 3$ W cm^{-2}, $I_R = 0$ (for one side incidence), $I_L = 1.5$ W cm^{-2}, $I_R = 1.5$ W cm^{-2} (for both sides incidence), $f = 2450$ MHz.

Fig. 9a–f illustrate the variations for t_p and ΔT_p vs. sample thickness (L_s) with/without support due to one side and both sides incidence. As mentioned earlier, it may be noted that the processing without any pulsing corresponds to case 1 and pulsing corresponds to cases 2 and 3 (refer Fig. 1c).

It is observed from Fig. 9a that, t_p is an increasing function till $L_s = 0.7$ cm and thereafter local minima occurs and further, t_p is found to be an increasing function with L_s.

An increasing trend of t_p vs. L_s is observed for $L_s \geq 1$ cm (one side incidence) and 1.5 cm (both sides incidence) with cases 2 and 3 for no support (Fig. 9a,b). It is also observed that t_p for one side incidence case is larger than that for both sides incidence with cases 2 and 3. Similar to WP samples, it is also observed that ΔT_p for case 3 is larger than that for case 2, but t_p for case 3 is smaller than for case 2 in all situations. Common to all these cases, it is observed that ΔT_p is a sharp increasing function of L_s especially for $L_s \geq 0.7$ cm with one side incidence and for $L_s \geq 1.7$ cm with both sides incidence with case 1 (no pulsing). As observed earlier in WP samples, application of pulsing drastically reduces ΔT_p for cases 2 and 3 for PLR samples. However, ΔT_p is found to have smaller magnitudes for $L_s \geq 0.9$ cm. Qualitatively similar distributions for t_p and ΔT_p are observed for alumina and SiC supports for one side and both sides microwave incidence (Fig. 9c–f). The detailed spatial characterization of power and temperature and pulsing characteristics are qualitatively similar as seen in Figs. 5 and 6 and thus they are not shown for PLR samples. Overall processing time, thermal runaway and optimal heating characteristics for various PLR sample thicknesses are discussed next.

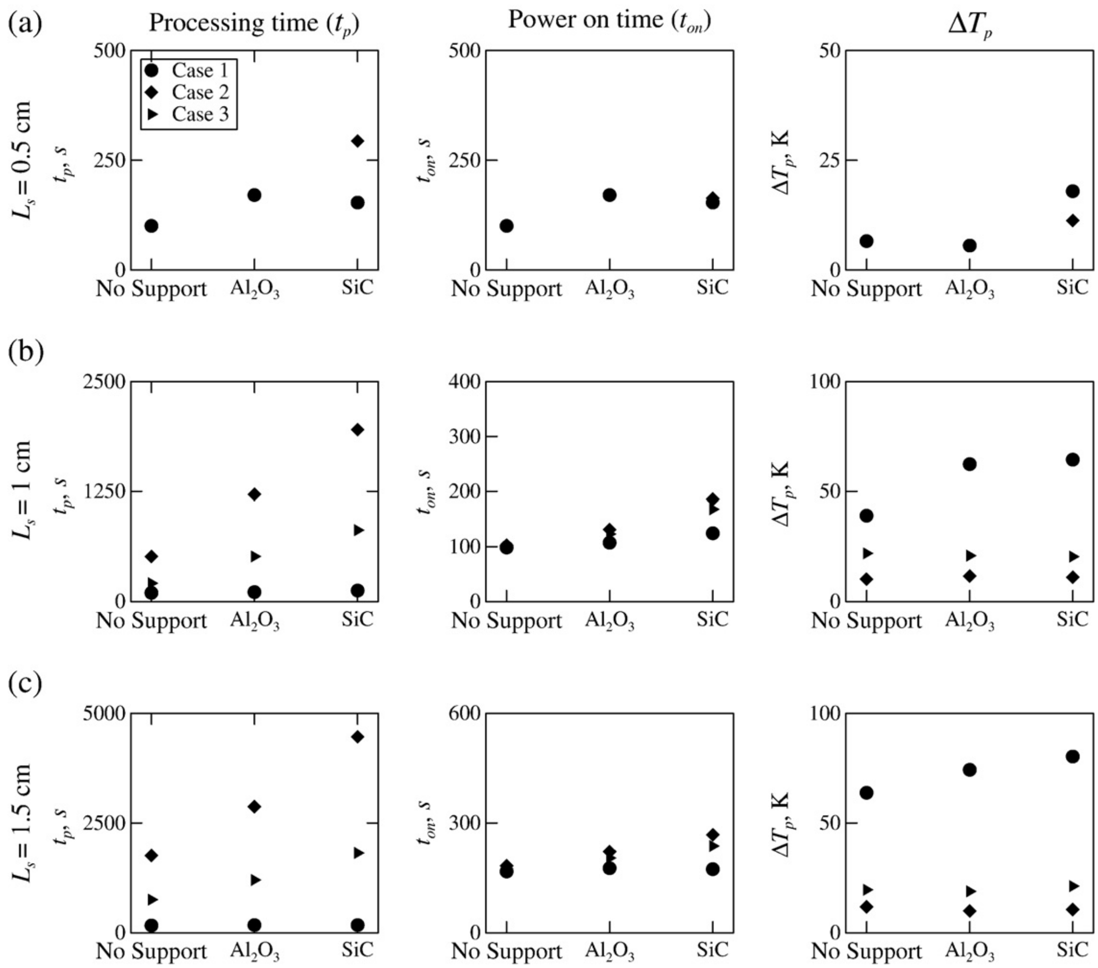

Fig. 8. Processing time (t_p), power on time (t_{on}) and temperature difference (ΔT_p) for White Pudding (WP) samples without plate and with alumina and SiC plates corresponding to cases 1–3 due to one side incidence: (a) $L_s = 0.5$ cm, (b) $L_s = 1$ cm and (c) $L_s = 1.5$ cm. $f = 2450$ MHz, $I_L = 3$ W cm^{-2}, $I_R = 0$, $T' = 2$ K.

Fig. 10a shows that both processing time (t_p), power on time (t_{on}) are largest for alumina support for $L_s = 0.5$ cm whereas smallest t_{on} is observed without any support. It is interesting to observe that t_{on} is almost identical with cases 1–3 for situations with no support or any support. Finally, it is observed that ΔT_p is minimum for alumina support irrespective of cases 1–3 and ΔT_p with no support has moderate values whereas maximum ΔT_p is observed for SiC support. Therefore, alumina support or no support with any case may be optimal choice for heating $L_s = 0.5$ cm sample based on t_p and ΔT_p values.

Fig. 10b illustrates that processing time (t_p), power on time (t_{on}) are largest for SiC support whereas samples without support correspond to smallest t_p and t_{on} for $L_s = 1$ cm. Although the processing time varies considerably for all the cases with/without support, but the power on time is almost invariant for all the cases (cases 1–3) with no support and alumina support, as seen in Fig. 10b. It may be observed that, samples with alumina, SiC supports or without support with cases 2–3 have less thermal runaway as compared to case 1, but samples without supports with cases 2 and 3 have significantly less both processing time (t_p) and thermal runaway (ΔT_p). It may be inferred that no support with case 2 or 3 may be suitable for $L_s = 1$ cm based on t_p, t_{on} and ΔT_p values.

Fig. 10c illustrates t_p, t_{on} and ΔT_p is observed for $L_s = 2$ cm. Similar qualitative trend on t_p, t_{on} and ΔT_p is observed for $L_s = 2$ cm and $L_s = 1$ cm corresponding to all cases with/without support (see Fig. 10b and c). Note that, processing time and power on time are largest for SiC support and smallest in absence of any support. It is interesting to observe that ΔT_p is significantly high for case 1 with/without support. It is also observed that, processing time is in general larger than $L_s = 0.5$ and 1 cm. It may be noted that, ΔT_p has identical values for each of cases 2 and 3 with/without support. Thus, either no support or alumina support with case 3 may be the optimal choice for larger sample thicknesses based on smaller power on time (t_{on}).

4. Conclusion

A detailed analysis has been carried out on microwave heating for meat (White Pudding and Pork Luncheon Roll) samples either attached with ceramic (alumina or SiC) plate or without any plate corresponding to continuous and pulsed microwave incidences at one side and both sides. The coupled energy balance equation and the electric field equations based on temperature dependent dielectric and thermal properties are solved using Galerkin finite element method. The heating strategy for various length scales of pork meat samples has been investigated via pulsed microwave heating strategy based on processing time, microwave power on time and temperature difference characteristics either for one side or both sides microwave incidences (cases 1–3). The processing time and temperature difference are found to be a strong function of ceramic support, sample thickness, setpoint, on–off constraint and type of microwave distribution (one side and both sides incidence). Spatial power distribution is strongly coupled with spatial temperature distribution

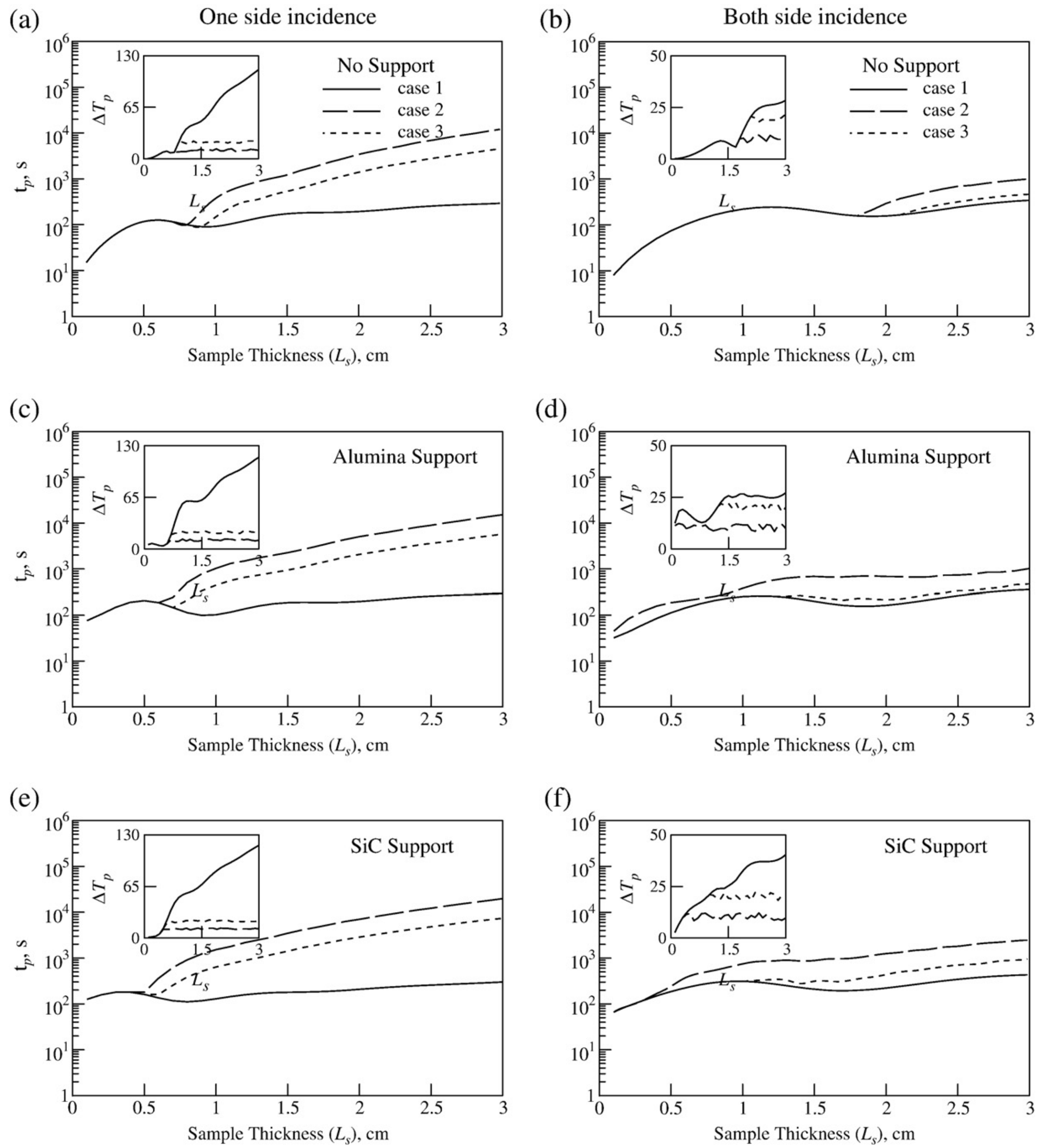

Fig. 9. Processing time (t_p) and temperature difference (ΔT_p) vs. sample thickness (L_s) diagrams for cases 1–3, corresponding to without plate, alumina and SiC plates for Pork Luncheon Roll (PLR) due to one side (a, b and c) and both sides (d, e and f) incidence. $I_L = 3$ W cm^{-2}, $I_R = 0$ W cm^{-2} (for one side incidence), $I_L = 1.5$ W cm^{-2}, $I_R = 1.5$ W cm^{-2} (for both sides incidence), $f = 2450$ MHz, $T' = 2$ K.

during power on period as dielectric properties of the meat are strong functions of temperature especially at $T \leq 358$ K.

Overall heating characteristics, role of pulsing and supporting plate and optimal thermal runaway policies for microwave heating of two meat batters are summarized below:

- The spatial hot spots occur either at the center or the outer face of the sample or at the face attached with alumina plate and pulsing plays a critical role to minimize hot spot formation or thermal runaway.
- Pulsing is carried out with two parameters: temperature constraint for on–off control (T') and set point for temperature difference (ΔT_S). Choice of T' and ΔT_S play a crucial factor for efficient pulsed microwave heating. The effect of T' becomes significant as the sample thickness increases.
- It is observed that power off time is larger for thick samples compared to thin samples.
- Higher ΔT_S and lower T' for thick meat samples may be preferred whereas lesser ΔT_S is suitable for thin meat samples.
- It is found that, alumina plate with case 3 ($\Delta T_S = 20$ K) may be optimal for both thin and thick meat samples.
- Overall processing time is larger for PLR with one/both side microwave incidence compared to WP samples.
- It is also observed that SiC plate may be selectively used and the optimal heating effects would occur with $\Delta T_S = 20$ K for both the pork meats (WP and PLR).
- It is also interesting to observe that degree of thermal runaway is lesser even without pulsing for distributed microwave incidence and thus processing time is in general less for distributed incidence for both pork meat substances (WP and PLR).

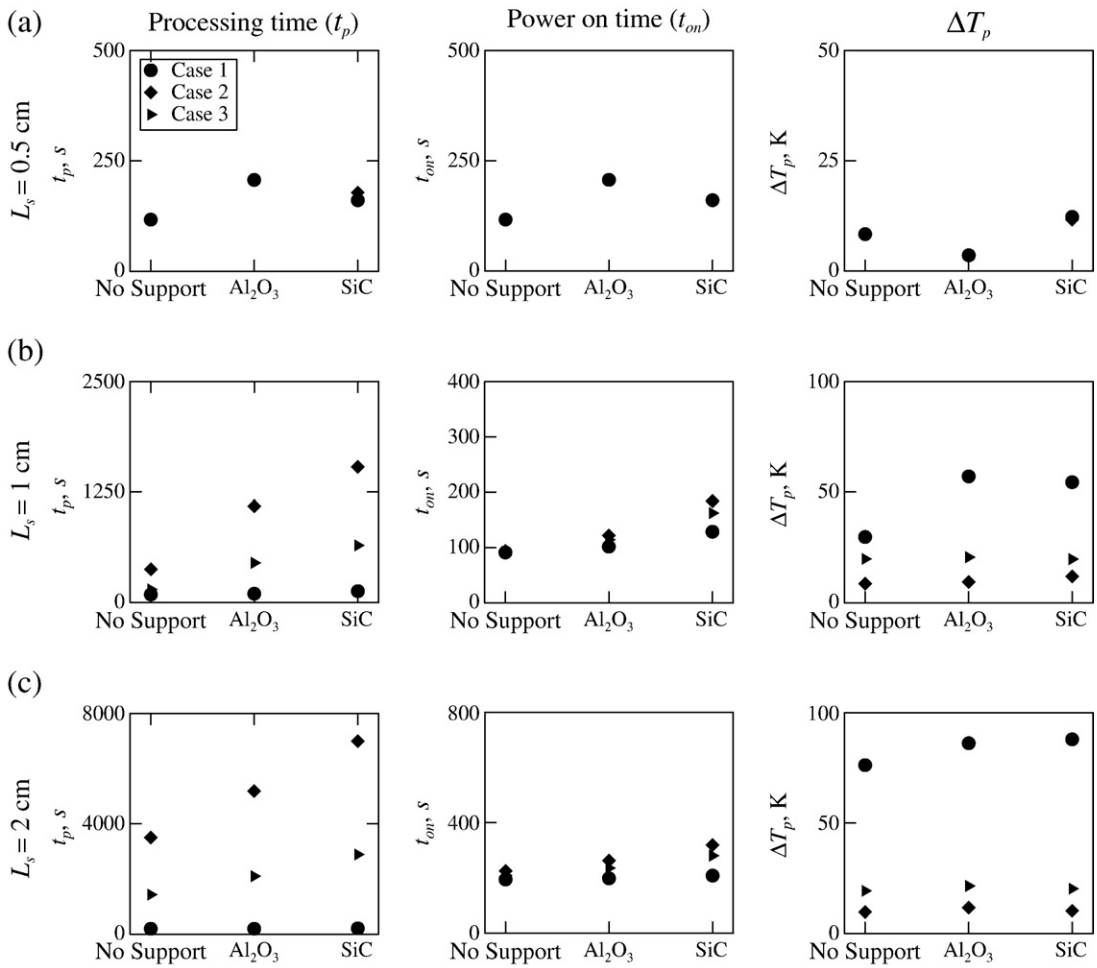

Fig. 10. Processing time (t_p), power on time (t_{on}) and temperature difference (ΔT_p) for Pork Luncheon Roll (PLR) samples without plate and with alumina and SiC plates corresponding to cases 1–3 due to one side incidence: (a) $L_s = 0.5$ cm, (b) $L_s = 1$ cm and (c) $L_s = 1.5$ cm. $f = 2450$ MHz, $I_L = 3$ W cm^{-2}, $I_R = 0$, $T' = 2$ K.

Till date, experimental investigations on microwave heating within meat slabs with or without supports in presence of uniform plane microwave is yet to appear in the literature. Current results based on uniform plane wave propagation are useful to carry out experiments in custom single mode microwave ovens. In addition, optimal heating situations of WP and PLR samples with various supports in presence of pulsing microwave incidence may be further verified with experiments in custom microwave ovens, which may be a subject of future research. Current theoretical analysis may also be applied to study heating of various discrete samples composited with ceramic plates in presence of pulsing of microwaves.

Notations

C_p	specific heat capacity, J kg^{-1} K^{-1}
c	velocity of light, m s^{-1}
E_x	electric field intensity, V m^{-1}
f	frequency, Hz
H	enthalpy, J m^{-3}
h	heat transfer coefficient, W m^{-2} K^{-1}
k	thermal conductivity, W m^{-1} K^{-1}
L	half-slab thickness, m
L_s	sample thickness, m
q	microwave source term, W m^{-3}
t	time, s
t_p	total processing time, s
t_{on}	power on time, s
t_{off}	power off time, s
T	temperature, K
T_0	initial temperature, K
T_∞	ambient temperature, K
T'	on–off constraint, K
ΔT_p	temperature difference within the sample, K
ΔT_S	setpoint for temperature difference, K
ΔT_{on}	setpoint for power on, K
$\overline{T}$	average temperature, K
z	distance, m

Greek symbols

ε_0	free space permittivity, F m^{-1}
κ	propagation constant
κ'	relative dielectric constant
κ''	relative dielectric loss
κ	relative complex dielectric properties
ρ	density, kg m^{-3}
ω	angular frequency, Rad s^{-1}

Subscripts

l	layer number

Acknowledgment

Authors would like to thank anonymous reviewers for critical comments and suggestions which improved the quality of the manuscript.

References

Alajaji, S. A., & El-Adawy, T. A. (2006). Nutritional composition of chickpea microwave cooking and other (*Cicer arietinum* L.) as affected by traditional cooking methods. *Journal of Food Composition and Analysis*, *19*(8), 806−812.

Ayappa, K. G., Davis, H. T., Crapiste, G., Davis, E. A., & Gordon, J. (1991). Microwave-heating — An evaluation of power formulations. *Chemical Engineering Science*, *46*(4), 1005−1016.

Ayappa, K. G., Davis, H. T., Davis, E. A., & Gordon, J. (1991). Analysis of microwave-heating of materials with temperature-dependent properties. *AIChE Journal*, *37*(3), 313−322.

Ayappa, K. G., Davis, H. T., Davis, E. A., & Gordon, J. (1992). Two-dimensional finite element analysis of microwave heating. *AIChE Journal*, *38*(10), 1577−1592.

Barringer, S. A., Davis, E. A., Gordon, J., & Ayappa, K. G. (1995). Microwave-heating temperature profiles for thin slabs compared to Maxwell and Lambert Law predictions. *Journal of Food Science*, *60*(5), 1137−1142.

Basak, T., & Kumaran, S. S. (2005). A generalized analysis on material invariant characteristics for microwave heating of slabs. *Chemical Engineering Science*, *60*(20), 5480−5498.

Basak, T., & Priya, A. S. (2005). Role of ceramic supports on microwave heating of materials.*Journal of Applied Physics*, *97*(8) Art. No. 083537.

Basak, T., & Meenakshi, A. (2006a). Influence of ceramic supports on microwave heating for composite dielectric food slabs. *AIChE Journal*, *52*(6), 1995−2007.

Basak, T., & Meenakshi, A. (2006b). A theoretical analysis on microwave heating of food slabs attached with ceramic plates: Role of distributed microwave incidence. *Food Research International*, *39*(8), 932−944.

Bhattacharya, M., & Basak, T. (2006). A novel closed-form analysis on asymptotes and resonances of microwave power. *Chemical Engineering Science*, *61*(19), 6273−6301.

Bonafonte, A. B., Iglesias, O., & Bueno, J. L. (2007). Effects of operating conditions on the combined convective–microwave drying of agar gels. *Drying Technology*, *25*(11), 1867−1873.

Brunton, N. P., Lyng, J. G., Zhang, L., & Jacquier, J. C. (2006). The use of dielectric properties and other physical analyses for assessing protein denaturation in beef biceps femoris muscle during cooking from 5 to 85 degrees C. *Meat Science*, *72*(2), 236−244.

Campanone, L. A., & Zaritzky, N. E. (2005). Mathematical analysis of microwave heating process. *Journal of Food Engineering*, *69*(3), 359−368.

Chatterjee, A., Basak, T., & Ayappa, K. G. (1998). Analysis of microwave sintering of ceramics. *AIChE Journal*, *44*(10), 2302−2311.

Chen, X. D. (1998). Microwave heating of an infinite solid slab and its thermal stability analysis using steady state bifurcation theory. *Journal of Food Engineering*, *35*(3), 339−349.

Curet, S., Rouaud, O., & Boillereaux, L. (2008). Microwave tempering and heating in a single-mode cavity: Numerical and experimental investigations. *Chemical Engineering and Processing: Process Intensification*, *47*(9–10), 1656−1665.

Damez, J. L., & Clerjon, S. (2008). Meat quality assessment using biophysical methods related to meat structure. *Meat Science*, *80*(1), 132−149.

Farag, K. W., Lyng, J. G., Morgan, D. J., & Cronin, D. A. (2008). Dielectric and thermophysical properties of different beef meat blends over a temperature range of −18 to +10 degrees C. *Meat Science*, *79*(4), 740−747.

Garg, V., & Mendiratta, S. K. (2006). Studies on tenderization and preparation of enrobed pork chunks in microwave oven. *Meat Science*, *74*(4), 718−726.

Gunasekaran, S., & Yang, H. W. (2007a). Effect of experimental parameters on temperature distribution during continuous and pulsed microwave heating. *Journal of Food Engineering*, *78*(4), 1452−1456.

Gunasekaran, S., & Yang, H. W. (2007b). Optimization of pulsed microwave heating. *Journal of Food Engineering*, *78*(4), 1457−1462.

Hill, J. M., & Marchant, T. R. (1996). Modelling microwave heating. *Applied Mathematical Modelling*, *20*(1), 3−15.

Jeong, J. Y., Lee, E. S., Choi, J. H., Lee, J. Y., Kim, J. M., Min, S. G., Chae, Y. C., & Min, C. J. (2007). Variability in temperature distribution and cooking properties of ground pork patties containing different fat level and with/without salt cooked by microwave energy. *Meat Science*, *75*(3), 415−422.

Khraisheh, M. A. M., Cooper, T. J. R., & Magee, T. R. A. (1995). Investigation and modeling of combined microwave and air-drying. *Food and Bioproducts Processing*, *73*(C3), 121−126.

Kwon, J. H., Belanger, J. M. R., Pare, J. R. J., & Yaylayan, V. A. (2003). Application of the microwave-assisted process (MAP (TM)) to the fast extraction of ginseng saponins. *Food Research International*, *36*(5), 491−498.

Lin, Y. E., Anantheswaran, R. C., & Puri, V. M. (1995). Finite element analysis of microwave heating of solid foods. *Journal of Food Engineering*, *25*(1), 85−112.

Liu, C. M., Wang, Q. Z., & Sakai, N. (2005). Power and temperature distribution during microwave thawing, simulated by using Maxwell's Equations and Lambert's Law. *International Journal of Food Science and Technology*, *40*(1), 9−21.

Lyng, J. G., Zhang, L., & Brunton, N. P. (2005). A survey of the dielectric properties of meats and ingredients used in meat product manufacture. *Meat Science*, *69*(4), 589−602.

Lyng, J. G., Cronin, D. A., Brunton, N. P., Li, W. Q., & Gu, X. H. (2007). An examination of factors affecting radio frequency heating of an encased meat emulsion. *Meat Science*, *75*(3), 470−479.

McKenna, B. M., Lyng, J., Brunton, N., & Shirsat, N. (2006). Advances in radio frequency and ohmic heating of meats. *Journal of Food Engineering*, *77*(2), 215−229.

McMinn, W. A. M. (2004). Prediction of moisture transfer parameters for microwave drying of lactose powder using Bi–G drying correlation. *Food Research International*, *37*(10), 1041−1047.

McMinn, W. A. M. (2006). Thin-layer modelling of the convective, microwave, microwave–convective and microwave–vacuum drying of lactose powder. *Journal of Food Engineering*, *72*(2), 113−123.

McMinn, W. A. M., Khraisheh, M. A. M., & Magee, T. R. A. (2003). Modelling the mass transfer during convective, microwave and combined microwave–convective drying of solid slabs and cylinders. *Food Research International*, *36*(9–10), 977−983.

Ng, S. K., Ainsworth, P., Plunkett, A., Haigh, A. D., Gibson, A. A. P., Parkinson, G., & Jacobs, G. (2008). Determination of added fat in meat paste using microwave and millimetre wave techniques. *Meat Science*, *79*(4), 748−756.

Ohlsson, T., & Bengtsson, N. E. (1971). Microwave heating profiles in foods: A comparison between heating experiments and computer simulation. *Microwave Energy Applications Newsletter*, *4*(6), 3−8.

Oliveira, M. E. C., & Franca, A. S. (2002). Microwave heating of foodstuffs. *Journal of Food Engineering*, *53*(4), 347−359.

Rahman, S. (1995). *Food properties handbook.* Boca Raton: CRC Press Inc.

Ramaswamy, H. S., & Pilletwill, T. (1992). Temperature distribution in microwave-heated food models. *Journal of Food Quality*, *15*(6), 435−448.

Regier, M., Housova, J., & Hoke, K. (2001). Dielectric properties of mashed potatoes. *International Journal of Food Properties*, *4*(3), 431−439.

Rodriguez, E. M. T., Penazzi, G., Caboni, M. F., Bertscco, G., & Lercker, G. (1997). Effect of different cooking methods on some lipid and protein components of hamburgers. *Meat Science*, *45*(3), 365−375.

Sanz, P. D., Alonso, M. D., & Mascheroni, R. H. (1987). Thermophysical properties of meat products: General bibliography and experimental values. *Transactions of the ASAE*, *30*(1), 283−296.

Serrano, A., Librelotto, J., Cofrades, S., Sanchez-Muniz, F. J., & Jimenez-Colmenero, F. (2007). Composition and physicochemical beef steaks containing walnuts as characteristics of restructured affected by cooking method. *Meat Science*, *77*(3), 304−313.

Taher, B. J., & Farid, M. M. (2001). Cyclic microwave thawing of frozen meat: experimental and theoretical investigation. *Chemical Engineering and Processing*, *40*(4), 379−389.

Vasanthi, C., Venkataramanujam, V., & Dushyanthan, K. (2007). Effect of cooking temperature and time on the physico-chemical, histological and sensory properties of female carabeef (buffalo) meat. *Meat Science*, *76*(2), 274−280.

Wang, J., Binner, J., Vaidhyanathan, B., Joomun, N., Kilner, J., Dimitrakis, G., & Cross, T. E. (2006). Evidence for the microwave effect during hybrid sintering. *Journal of American Ceramic Society*, *89*(6), 1977−1984.

Wang, L. J., & Sun, D. W. (2003). Recent developments in numerical modelling of heating and cooling processes in the food industry — A review. *Trends in Food Science and Technology*, *14*(10), 408−423.

Yang, H. W., & Gunasekaran, S. (2001). Temperature profiles in a cylindrical model food during pulsed microwave heating. *Journal of Food Engineering*, *66*(7), 998−1004.

Yang, H. W., & Gunasekaran, S. (2004). Comparison of temperature distribution in model food cylinders based on Maxwell's Equations and Lambert's Law during pulsed microwave heating. *Journal of Food Engineering*, *64*(4), 445−453.

Yarmand, M. S., & Homayouni, A. (2009). Effect of microwave cooking on the microstructure and quality of meat in goat and lamb. *Food Chemistry*, *112*(4), 782−785.

Zhang, L., Lyng, J. G., Brunton, N., Morgan, D., & McKenna, B. (2004). Dielectric and thermophysical properties of meat batters over a temperature range of 5–85 degrees C. *Meat Science*, *68*(2), 173−184.